

Figure S1 related to figure 1

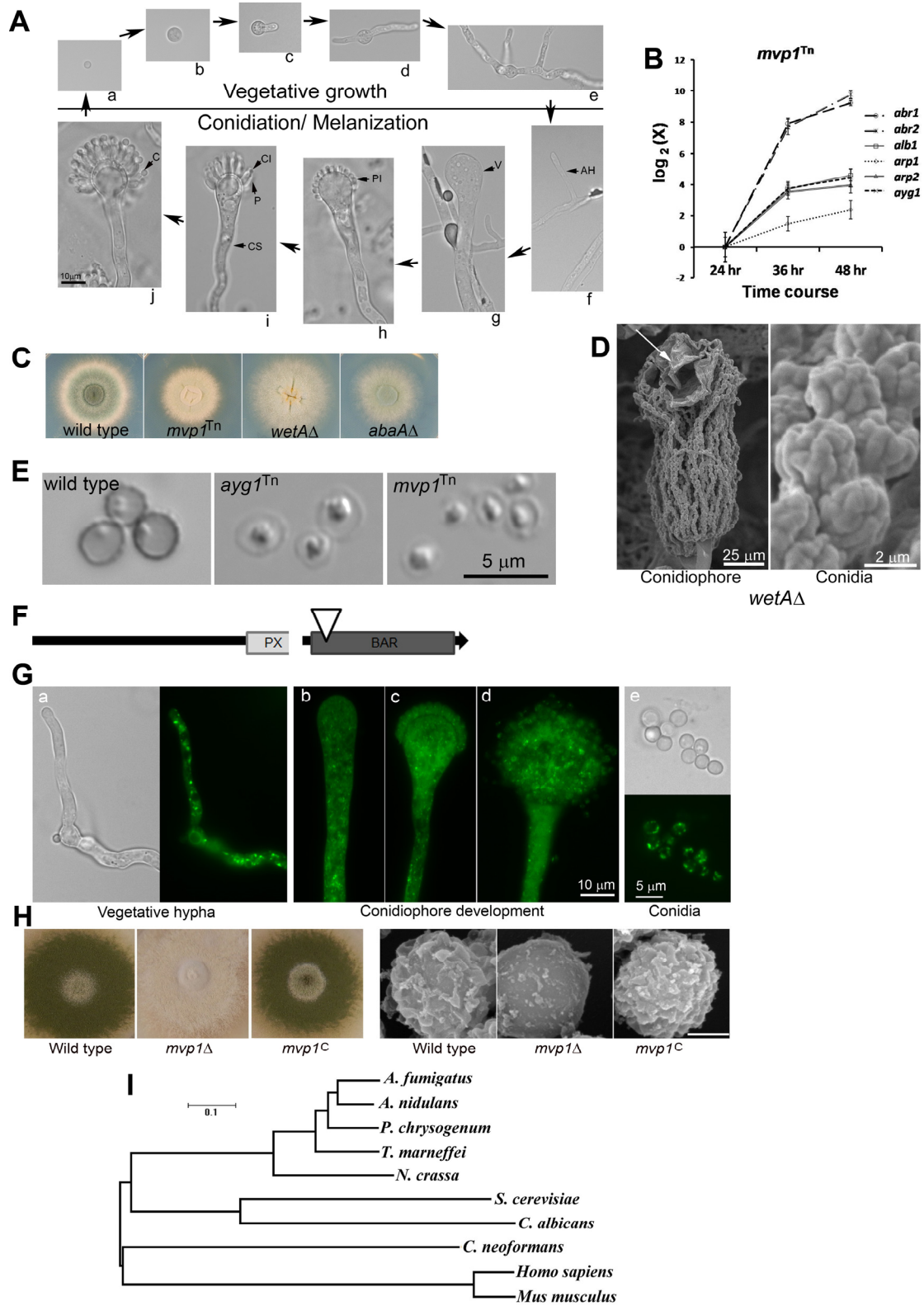


Figure S1. The asexual life cycle of *A. fumigatus* and Mvp1. (A) Development of *A. fumigatus* from a dormant conidium [a], germinating conidium [b], germ tube [c], young vegetative hypha [d], competent hypha [e], aerial hypha/AH [f], conidiophore stalk or vesicle/V [g], to a conidiophore with phialide initiation/PI [h], with phialide /P and conidial initiation/CI [i], and with mature conidia/C [j]. Melanization only occurs during conidiation process. (B) The expression of the melanin biosynthetic genes *alb1*, *ayg1*, *arp1*, *arp2*, and *abr1*, and *abr2* in the *mvp1*^{Tn} mutant during conidiation. The induction is similar to what we previously observed in the wild type (Upadhyay et al., 2013). (C) Colony images of the wild type, the *mvp1*^{Tn} mutant, the *abaA*Δ mutant, and the *wetA*Δ mutant. (D) SEM images of the conidiophore (left) and conidia (right) of the *wetA*Δ mutant. Conidial lysis in the *wetA*Δ mutant causes the accumulation of lysate (white arrow) on conidiophores and the appearance of deflated conidia. (E) Images of digested conidia from wild type, the *ayg1*^{Tn} melanin mutant, and the *mvp1*^{Tn} mutant. (F) A diagram of Mvp1 domain structures and the Ti plasmid insertion site (white triangle) in the *mvp1*^{Tn} mutant. BAR: Bin-Amphiphysin-Rvs domain for oligomerization and curving membranes. PX: PHOX domain recognizing phosphatidylinositol 3-phosphate. (G) Mvp1-GFP localization at different development stages. [a] vegetative hypha, [b] stalk, [c] young conidiophore, [d] mature conidiophore, [e] conidia. (H) Colony (left) and conidial SEM (right) images of *A. nidulans* wild type, the *mvp1*Δ mutant, and the complemented strain (*MVP1*^C). Scale bar: 1 μm. (I) Phylogenetic relationship among Mvp1 proteins in different organisms: *A. fumigatus*, *A. nidulans*, *Penicillium chrysogenum*, *Talaromyces marneffeii*, *Neurospora crassa*, *Saccharomyces cerevisiae*, *Candida albicans*, *Cryptococcus neoformans*, *Homo sapiens* (SNX8/Mvp1), and *Mus musculus* (SNX8/Mvp1).

Figure S2 related to figure 2

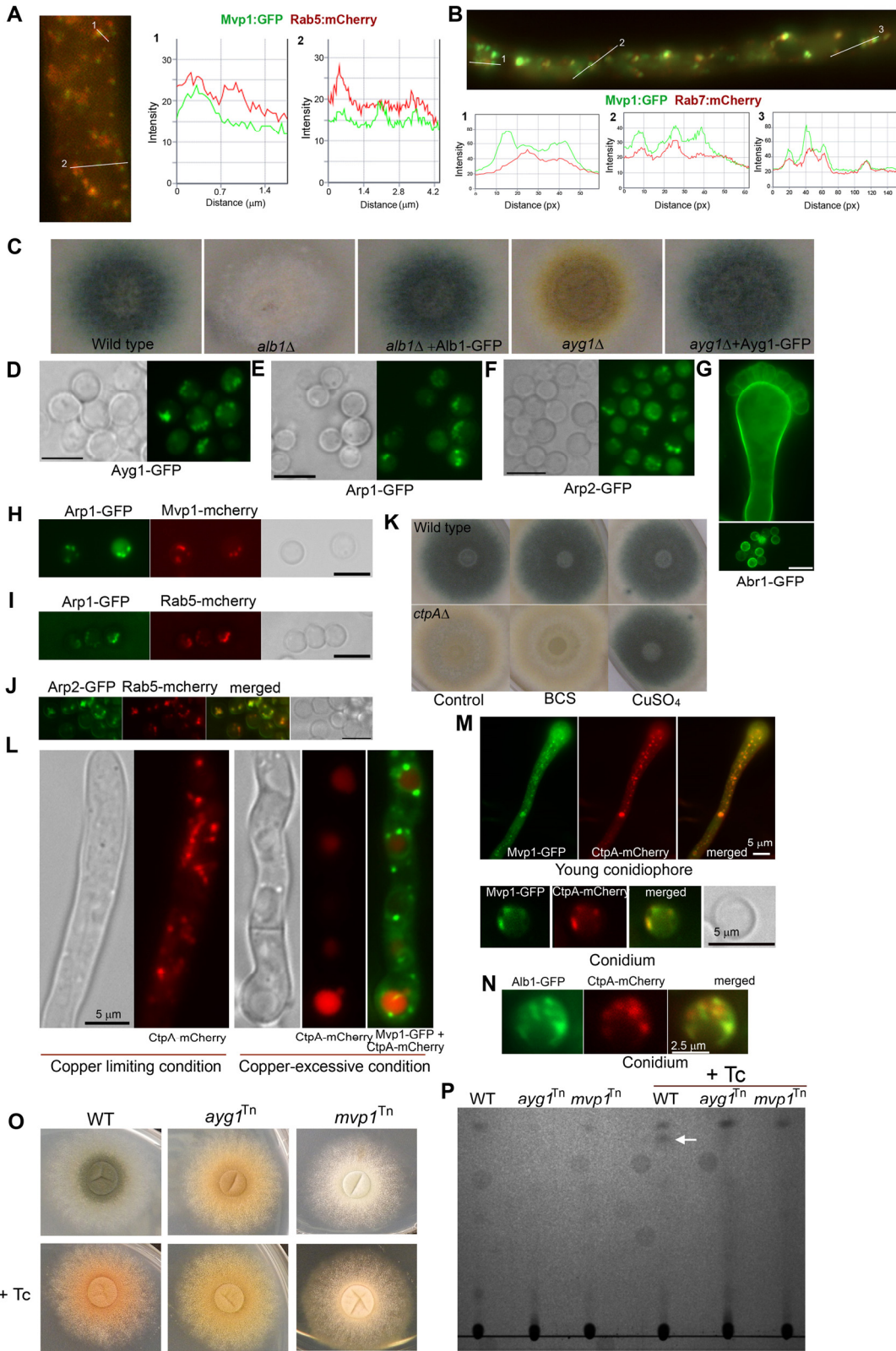


Figure S2. Localization of melanin enzymes, Mvp1, and the copper transporter CtpA. (A)

The image of merged Mvp1-GFP and Rab5-mCherry is identical to the one in Fig. 2C. The fluorescence intensity profile is plotted against the distance along the lines 1 and 2 shown in the image to the left. Plot 1 shows a peak with Rab5 but not with Mvp1. Plot 2 shows a Mvp1 peak without a corresponding peak of Rab5. **(B)** The image of merged Mvp1-GFP and Rab7-mCherry is identical to the one in Fig. 2D. The fluorescence intensity profile is plotted against the distance along the lines 1, 2 and 3 shown in the image on the top. Plot 1 shows two Mvp1 peaks without corresponding peaks of Rab7. Plot 2 shows one Mvp1 peak without a corresponding peak of Rab7. Plot 3 shows a very well overlapped peak from both Mvp1 and Rab7. **(C)** Restoration of pigmentation in the *alb1* Δ mutant by Alb1-GFP and in the *ayg1* Δ mutant by Ayg1-GFP. **(D)** Localization of the early melanin enzyme Ayg1. **(E)** Localization of the early melanin enzyme Arp1. **(F)** Localization of the early melanin enzyme Arp2. **(G)** Localization of the late enzyme Abr1. **(H)** Localization of Arp1 and Mvp1. **(I)** Localization of Arp1 and the endosomal marker Rab5. **(J)** Localization of Arp2 and the endosomal marker Rab5. Scale bars: 5 μ m. **(K)** Colony images showing the pigmentation defect of the *ctpA* Δ mutant under copper-limiting conditions. The wild type and the *ctpA* Δ mutant were grown on CM medium, CM+BCS (copper chelator), and CM+copper. **(L)** Localization of CtpA-mCherry under a copper-limiting condition (left). Localization of CtpA-mCherry under copper excessive condition (right) in a strain expressing Mvp1-GFP. The CtpA-mCherry was localized to vacuoles under the copper-replete condition. **(M)** Localization of Mvp1-GFP and CtpA-mCherry in a young conidiophore (top) and conidia (bottom). **(N)** Localization of the early melanin enzyme Alb1-GFP and the copper transporter CtpA-mCherry. **(O)** Colony images of wild type *A. fumigatus*, the *ayg1*^{Tn} melanin mutant, and the *mvp1*^{Tn} melanin mutant with or without the

treatment of tricyclazole. Tc: tricyclazole. Tricyclazole specifically inhibits reductases like Arp2 and causes the accumulation of the shunt product flaviolin derived from the intermediate 1,3,6,8-THN, which is produced by the Ayl1-catalyzed reaction (Tsai et al., 2001). Thus, tricyclazole treatment rendered WT reddish orange, similar to the *arp2* mutant (see Figure 1A)(Jackson et al., 2009; Tsai et al., 2001). Tricyclazole treatment did not affect the *ayg1*^{Tn} mutant, which remained its yellow color. This is because the *ayg1*^{Tn} mutant does not produce 1,3,6,8-THN that can be converted to flaviolin (Jackson et al., 2009; Tsai et al., 2001). Tricyclazole treatment altered the *mvp1*^{Tn} mutant only slightly. This is consistent with predicted low level of early melanin intermediates in this *mvp1*^{Tn} mutant. (P) Thin layer chromatography of extracts from conidia collected from cultures of wild type *A. fumigatus*, the *ayg1*^{Tn} melanin mutant, and the *mvp1*^{Tn} melanin mutant with or without tricyclazole treatment. We observed the appearance of a new product in WT with tricyclazole treatment (white arrow), presumably flaviolin. As expected, that product was not detected in the *ayg1*^{Tn} mutant with tricyclazole treatment. We did not detect that product in the *mvp1*^{Tn} mutant, consistent with the predicted low level of melanin intermediates in this strain.

Figure S3 related to figure 4

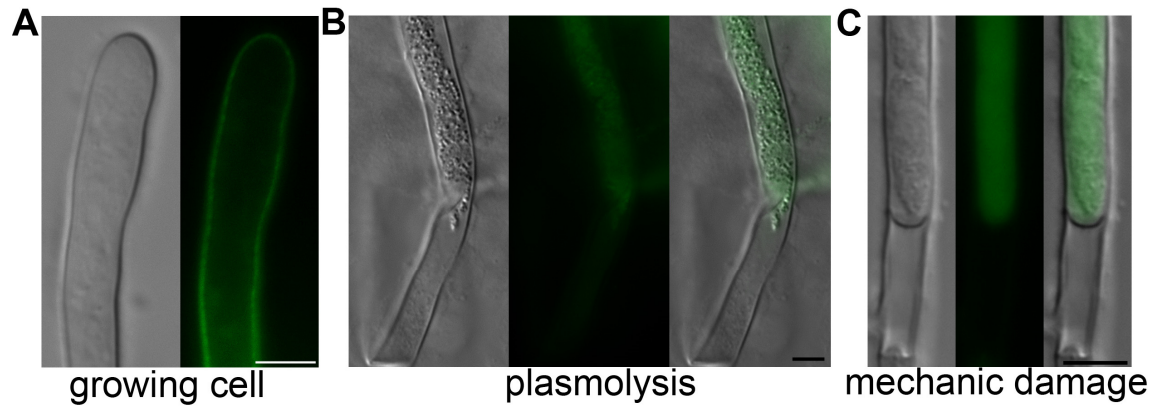


Figure S3. Behavior of the plasma-membrane located GFP-SsoA during active growth, plasmolysis, or mechanic severing. (A) GFP-SsoA is localized to plasma membrane during hyphal growth. (B) Plasmolysis of hyphae reveals intracellular localization of GFP-SsoA and its association with cytoplasm. (C) Mechanic severing of the hyphae reveals the association of GFP-SsoA with cytoplasm in the intact hyphal cell neighboring the damaged hyphal cell (bottom). The region where cytoplasm is absent in the intact cell also shows no SsoA-GFP signal. The septum is near the bottom of the images. Scale bars: 5 μ m.

Supplemental Tables

Table S1. Strains used in this study.

Strains	Genotype	Source
CEA10	Wild-type	FGSC
CEA17	<i>pyrG1</i>	FGSC
A293	Wild-type	FGSC
ASUC1	<i>pyrG1</i> , Δ <i>ctpA::hph</i>	(Upadhyay et al., 2013)
TSGa17	<i>AfupyrG1</i> ; Δ <i>AfuabaA::AfupyrG+</i>	(Tao and Yu, 2011)
TSGw4	<i>AfupyrG1</i> ; Δ <i>AfuwetA::AfupyrG+</i>	(Tao and Yu, 2011)
Δ abr1	Δ <i>abr1::hph</i>	(Tsai et al., 1999)
Δ abr1.2	Δ <i>abr1::hph</i> , <i>AfupyrG2</i>	This study
Δ abr2	Δ <i>abr2::hph</i>	(Tsai et al., 1999)
Δ abr2.2	Δ <i>abr2::hph</i> , <i>AfupyrG2</i>	This study
Δ alb1	Δ <i>alb1::hph</i>	(Tsai et al., 1999)
Δ alb1.2	Δ <i>alb1::hph</i> , <i>AfupyrG2</i>	This study
Δ ayg1	Δ <i>ayg1::hph</i>	(Tsai et al., 1999)
Δ ayg1.2	Δ <i>ayg1::hph</i> , <i>AfupyrG2</i>	This study
Δ arp1	Δ <i>arp1::hph</i>	(Tsai et al., 1999)
Δ arp1.2	Δ <i>arp1::hph</i> , <i>AfupyrG2</i>	This study
Δ arp2	Δ <i>arp2::hph</i>	(Tsai et al., 1999)
Δ arp2.2	Δ <i>arp2::hph</i> , <i>AfupyrG2</i>	This study
AsuG1	<i>pyrG1</i> , <i>P_{abrA}-abrA-eGFP-AfupyrG</i>	(Upadhyay et al., 2013)
AsuG2	Δ <i>abr1::hph</i> , <i>AfupyrG2</i> , <i>P_{abrA}-abrA-eGFP-AfupyrG</i>	(Upadhyay et al., 2013)
AsuCG1	<i>pyrG1</i> , Δ <i>ctpA::hph</i> , <i>P_{ctpA}-ctpA-eGFP-AfupyrG</i>	(Upadhyay et al., 2013)
<i>mvp^{Tn}</i>	<i>mvp^{Tn}::hph</i> , <i>AfupyrG2</i>	(Jackson et al., 2009)
AsuG1	<i>pyrG1</i> , <i>P_{abrA}-abrA-eGFP-AfupyrG</i>	(Upadhyay et al., 2013)
AsuG2	Δ <i>abr1::hph</i> , <i>AfupyrG2</i> , <i>P_{abrA}-abrA-eGFP-AfupyrG</i>	(Upadhyay et al., 2013)
AsuCG1	<i>pyrG1</i> , Δ <i>ctpA::hph</i> , <i>P_{ctpA}-ctpA-eGFP-AfupyrG</i>	(Upadhyay et al., 2013)
AsuG3	<i>pyrG1</i> , <i>P_{abr2}-abr2-eGFP-AfupyrG</i>	This study
AsuG4	<i>pyrG1</i> , <i>P_{alb1}-alb1-eGFP-AfupyrG</i>	This study
AsuG5	Δ <i>alb1::hph</i> , <i>AfupyrG2</i> , <i>P_{alb1}-alb1-eGFP-AfupyrG</i>	This study
AsuG6	<i>pyrG1</i> , <i>P_{ayg1}-ayg1-eGFP-AfupyrG</i>	This study
AsuG7	Δ <i>ayg1::hph</i> , <i>AfupyrG2</i> , <i>P_{ayg1}-ayg1-eGFP-AfupyrG</i>	This study
AsuG8	<i>pyrG1</i> , <i>P_{arp1}-arp1-eGFP-AfupyrG</i>	This study
AsuG9	<i>pyrG1</i> , <i>P_{arp2}-arp2-eGFP-AfupyrG</i>	This study
AsuG10	<i>pyrG1</i> , <i>P_{mvp1}-mvp1-eGFP-AfupyrG</i>	This study
AsuG11	<i>pyrG1</i> , <i>P_{rab5}-mCherry-rab5</i> , <i>hph</i>	This study
AsuG12	<i>pyrG1</i> , <i>P_{rab7}-rab7-mCherry-hph</i>	This study
AsuG13	<i>pyrG1</i> , <i>P_{abrA}-abrA-eGFP-AfupyrG</i> , <i>P_{mvp1}-mvp1-mCherry-hph</i>	This study
AsuG14	<i>pyrG1</i> , <i>P_{abrA}-abrA-eGFP-AfupyrG</i> , <i>P_{abr2}-abr2-mCherry-hph</i>	This study
AsuG15	<i>pyrG1</i> , <i>P_{alb1}-alb1-eGFP-Afupyr</i> , <i>P_{rab5}-mCherry-rab5</i> , <i>hph</i>	This study

AsuG16	<i>pyrG1, P_{alb1}-alb1-eGFP-Afupyr, P_{mvp1}-mvp1-mCherry-hph</i>	This study
AsuG17	<i>pyrG1, P_{alb1}-alb1-eGFP-Afupyr, P_{ctpA}-ctpA-mCherry-hph</i>	This study
AsuG18	<i>pyrG1, P_{arp2}-arp2-eGFP-AfupyrG, P_{rab5}-mCherry-rab5, hph</i>	This study
AsuG19	<i>pyrG1, P_{mvp1}-mvp1-eGFP-AfupyrG, P_{ctpA}-ctpA-mCherry-hph</i>	This study
AX59	Δ <i>mvp::pyrG, pyroA4, pabaA1, pyrG89</i>	This study
AX62	<i>P_{mvp1}-mvp1-chRFP-pyroA, Δmvp::pyrG, pabaA1, pyroA4,</i>	This study
AX63	<i>P_{yA}-yA-chRFP-pyroA, pyrG89, pabaA1, pyroA4</i>	This study
AX66	<i>P_{yA}-chRFP- pyroA, yA1, argB2, pabaA1, pyroA4</i>	This study
AX70	<i>P_{yA}-yA-chRFP-pyroA, Δmvp1::pyrG, pabaA1, pyroA4,</i>	This study
AX78	<i>P_{wA}-wA-chRFP-pyroA, pyrG89, pyroA4, wA3</i>	This study
AX79	<i>P_{wA}-wA-chRFP-pyroA, pyrG, pabaA, pyroA4</i>	This study
AX110	<i>P_{wA}-wA-chRFP-pyroA, mvp1::pyrG, pabaA, pyroA4</i>	This study
Ax224	<i>P_{ALB1}-Alb1-GFP::PyrG, P_{BMH1}-BMH1-mCherry::Hygr</i>	This study
Ax226	<i>P_{ALB1}-Alb1-GFP::PyrG, P_{BMH2}-BMH2-mCherry::Hygr</i>	This study
Ax230	<i>P_{ARP2}-ARP2-GFP::PyrG, P_{BMH1}-BMH1-mCherry::Hygr</i>	This study
Ax232	<i>P_{ARP2}-ARP2-GFP::PyrG, P_{BMH2}-BMH2-mCherry::Hygr</i>	This study

FGSC: Fungal Genetics Stock Center (<http://www.fgsc.net/>)

Table S2. Oligonucleotides used in this study.

Primers	Sequence (5'→ 3')	Primers	Sequence (5'→ 3')
LB-B01	CGTCCGCAATGTGTTATTAAG	GFPnesR	GGTCGACTTGTCCCTGAGG
M13R	CAGGAAACAGCTATGAC	abr1nesF	CCTGTCTACCGAGATACAT
M13F	GTAAAACGACGGCCAG	abr2GFPnes	GAGCTAGTAAAGGAGTCG
AI76	AACAGTTGCGCAGCCTGAATG	ayg1GFPF1	CTGATCATTGCGCATCTGA
LB-UI	CCTCGGACGAGTGCTGG	rab5nesF	TCATCTCAGCCTGTTAGTG
AI77	AGAGGCGGTTTGCGTATTGG	rab5nesR	TCAGGTTCACTGGCTCA
TEF1Frtper	GTACCGGCAAGTCTGTTGA	wA4	TGGAGTGCAGTAACCAAG
TEF1Rrtper	ACGACACCAACAGCAACAG	wAF	CGTCTTGCTCGTGCATTTG
abr1Frtper	TGAGCAGGATGATTCACAAC	arp1GFPnes	GCCAAGAAGCCTTACTGA
abr1Rrtper	CAACTCCGAGTCGATAATCA	arp2GFPF1	TGACAGTTTGCAAGGTGCT
abr2Frtper	GTCTTCCAGCTGGTTGTCA	arp2GFPnes	TGATGGTGGCCAATGACCT
abr2Rrtper	TTGAGGTCCAGTTGAACTTG	alb1GFPF1	TGACCGACAGTCTCAACTT
alb1Frtper	TGAGCAGGATGATTCACAAC	ayg1GFPne	ACTGCGTGTACGGAGTGT
alb1Rrtper	CAACTCCGAGTCGATAATCA	arp1GFPF1	CAGACTGCATCTATCGGCC
ayg1Frtper	CTCCATCGAGGACTTTGAG	alb1GFPnes	TTGATCTGGAATCGTCCGT
ayg1Rrtper	GGGAGATGCGGTAGACAA	alb1GFPnes	AGTGATCACTTTCCTGTTT
arp1Frtper	CGTCAAGACCCAGCATCT	mCherryR1	ACAACCTTAATAACACATTG
arp1Rrtper	TCGACCTTGCGGTAGTAGT	mCherrynes	GTACTGAATTAACGCCGA
arp2Frtper	ACTTCAACGAGGTGTTC AAT		
arp2Rrtper	AATTGAGGACATGAGGATCA		
GFP Forward	GGAGCTGGTGCAGGCGCTGG		
GFP Reverse	CTGTCTGAGAGGAGGCACTGATGCG		
abr2GFPF1	GAACTCGGCGTCTCTTTAAT		
abr2GFPR1	CCAGCGCCTGCACCAGCTCCCATAGGAGTGATCATGTCTG		
ayg1GFPR1	CCAGCGCCTGCACCAGCTCCGTTCTTCGTCTTCGAAGGCG		
arp1GFPR1	CCAGCGCCTGCACCAGCTCCGACTGATGGCTTCGCGGC		
arp2GFPR1	CCAGCGCCTGCACCAGCTCCGCATTCCAAATCCCCACCGG		
alb1GFPR1	CCAGCGCCTGCACCAGCTCCGGAACTCATGGCCGTGGCCA		
alb1GFPF2	TGGCCACGGCCATGAGTTCCGGAGCTGGTGCAGGCGCTGG		
alb1GFPR2	AAACCTAGGAACTCACCCCACTGTCTGAGAGGAGGCACTG		
alb1GFPF3	CAGTGCCTCCTCTCAGACAGTGGGGTGAGTTCCTAGGTTT		
alb1GFPR3	TGGAATACTCCCGGGCTAAA		
mvp1mCF1	TCGATAAGAGAGTCTACCAAGGAGTGTAGC		
mvp1mCR1	CAGCGCCTGCACCAGCTCCCTCGCCCAAAGGCATTCCTTC		
mvp1mCnesF1	GGATTGTACACCCTCGAACA		
mCherryF1	GCAGTGGAGCCTGTCGTTGGAGCTGGTGCAGGCGCT		
ctpAmCF1	ACTGAGTCAGACGGACGCCA		
ctpAmCR1	GCGCCTGCACCAGCTCCAACGACAGGCTCCACTGC		
ctpAmCnesF1	ATCGAGTCAAGCATTGCAGA		
rab7mCF1	TGATAGTCTTCCGGCGATGA		
rab7mCR1	CCAGCGCCTGCACCAGCTCCGCATAGCGTTCTCTGTTCAT		

rab7mCnesF1	GTGCGGATAAAGGAGTAGGG
rab5F1	TATTAACGGGAGCATGCAGG
rab5R1	CCTTGCTGACCATGGCCGGCGAGCCCAACTTTATGTGA
rab5mcF2	TAAAGTTGGGCTCGCCGGCCATGGTCAGCAAGGGCGAAGA
rab5mcR2	TTGGCGCTCGTTGAGTCAGAACCGCCTCCGCCTCCGCCCT
rab5F3	AGGGCGGAGGCGGAGGCGGTTCTGACTCAACGAGCGCCAA
rab5R3	CCTCGACAAAGTGGACTATC
pyrGF	TGGTACACCGCTATGTGAAG
pyrGR	CTGTCTGAGAGGAGGCACTGATG
anmvp1F	AGCATTGCACTGGTGGCATTG
anmvp1R	CTTCACATAGCGGTGTACCAGATAAGGCACAGGCAGCAGGATG
anmvp2F	CATCAGTGCCTCCTCTCAGACAGTTCTGAGGTCTTGACGAATCGTAGTC
anmvp2R	GCGGTCGCGAAGAGATGCTAG
anmvpnestF	GGCCGATGTCATGGAGGATTCAC
anmvpnestR	GTGAGCGGAGCAAACCTGCAAC
anyanestF	AAGCCACACCCGCTTTCTC
anyaF	CCACGGACCTGACAATTCTCGAC
anyaR	CCAGCGCCTGCACCAGCTCCAGAATCCCAAACATCAACCCCGTC
ribR	GAGCATAACCGTGTGACTTGG
pyroR	CAGCTTTTCAGAATTCGCGAGTGTCTAC
pyronestR	TCTACATAATGAAGGACAAATGCACAGAACAC
wA1	GTAACTTCATTGTTTCACCCGAAGG
wA2	CTTCACATAGCGGTGTACCATGCACAGCGTGCCATTTACAG
wA3	CAAGGTTCAAACCTAACCGTCAAATGGAGGATCTCCATCGCCTCTATC
wAR	CCAGCGCCTGCACCAGCTCCGACCAACCGGCGCTCACAAAC
wAnestF	AAGCCACTTTTCAGGTGGCTTTTG
wA1F	TCAGTAGCTAGTGATTCGTCGTCGAC
wA2F	GTAGACACTCGCGAATTCTGAAAAGCTGGCTTTGGTTTTGGCTTAGGTTT
wA2R	TCACAACAGAGAATGCAGCACTGG
wA1nestF	ATTCATTCAATGGTGACAGCTGTTCC
wA2nestR	AAGCCGACGTTGCAAACAAACAG
anyanestF	AAGCCACACCCGCTTTCTC
Bmh1F	TGGAGATAGGAGGGAGGGAG
Bmh1R	CCAGCGCCTGCACCAGCTCCTTCAGCGGGCTTCTCGCC
Bmh1nest	ACCCGAATAATCCCTCCCCTC
Bmh2F	AGGATGATGCCTTATTGGCGAC
Bmh2R	CCAGCGCCTGCACCAGCTCCAGACTCGGTAGGAGCAGGCTTG
Bmh2nest	CTTCACCTCTTTGGCTTCGCTG
abr2FrtPCR2	ATTGATTTGGATCATAAAAAGA
abr2FrtPCR3	TTGTGCCGGTTGTCTCTT
abr2RrtPCR2	TGTTGTCGTGTATGAATGAACT
abr2RrtPCR3	CTGCCAGTTTCCCATGTC

Supplemental Experimental Procedures

Strains and growth conditions

Strains and primers used in this study are listed in Table S1 and Table S2 respectively. Strains were grown on standard *Aspergillus* complete medium (CM) and minimal medium (MM) media at 30°C with appropriate supplements as described previously (Upadhyay et al., 2013). The addition of copper sulfate (500 µM) to the media was used to represent the copper excess conditions and the addition of the copper chelator bathocuproine disulphonate /BCS (150 µM) to the media was used to represent copper-limiting conditions as previously described (Upadhyay et al., 2013).

Gene expression analysis

For gene expression studies, RNA samples of the wild type and the *mvp1*^{Tn} mutant were collected from cultures at the 24-h, 36-h, and 48-h time points as previously described (Upadhyay et al., 2013). Three biologically independent experiments were conducted. SYBR FAST qPCR master mix (KAPA Biosystems, Wilmington, MA) was used for the real-time PCR, and the reactions were performed in an Eppendorf RealPlex 2 machine according to the manufacturer's instructions. The expression level of the house-keeping gene *tefA* of the same samples was used to normalize the gene expression levels as previously described (Upadhyay et al., 2013). Primer set alb1Frtpr and alb1Rrtpr was used for *alb1*; ayg1Frtpr and ayg1Rrtpr was used for *ayg1*; arp1Frtpr and arp1Rrtpr was used for *arp1*; arp2Frtpr and arp2Rrtpr was used for *arp2*; abr1Frtpr and abr1Rrtpr was used for *abr1*; four different primer sets (abr2Frtpr and abr2Rrtpr, abr2Frtpr2 and abr2Rrtpr2, abr2Frtpr3 and abr2Rrtpr3 and abr2Frtpr2 and

abr2RrtPCR3) were used for *abr2*; and tefFrtPCR and tefRrtPCR was used for *tefA*. The sequences of these primers are included in Table S2.

Melanin ghost extraction

Melanin ghosts from collected conidia were extracted and dry biomass were quantified as previously described (Butler et al., 2009; Chai et al., 2010; Eisenman et al., 2005). Melanin ghosts were examined under light microscopy or by transmission electron microscopy as described in the methods section of the manuscript.

Electron Microscopy

Sample preparation and analyses for SEM and TEM were performed using similar procedures as described previously (Beauvais et al., 2013; van de Meene et al., 2006). Briefly, for scanning electron microscopy, samples were suspended in 2% glutaraldehyde buffered with 0.1M sodium phosphate, pH 7.2 overnight at 4°C and then washed 3x in the same buffer. Secondary fixation was done with 1% osmium tetroxide in buffer for 1h at room temperature. The samples were washed 3x with diH₂O and adhered to poly-lysine coated coverslips, then washed and treated with an ascending series of acetone solutions leading to complete dehydration. Critical-point drying was done with a CPD-020 unit (Balzers-Union, Principality of Liechtenstein) using liquid carbon dioxide. The dried samples on coverslips were mounted on aluminum stubs and coated with approx. 10-12nm of gold-palladium using a Hummer II sputter coater (Technics, San Jose, CA). Analysis was done with a JSM-6300 scanning electron microscope (JEOL USA, Peabody, MA) operated at 15kV and images were captured with an IXRF Systems model 500 digital processor (IXRF Systems Inc., Austin, TX).

For transmission electron microscopy, samples (intact conidia or melanin ghosts, see Supplemental Experimental Procedures) were gently removed from tubes and placed directly in a 50% (v/v) solution of Spurr's epoxy resin (Spurr, 1969) in anhydrous acetone for eight hours with rotation. The samples were then transferred to 3 consecutive changes of pure Spurr's over a period of approximately 30 hours under continual rotation and embedded in BEEM capsules. Resin blocks were polymerized for 24 hrs at 60°C. Thin sections were cut with an Ultracut-R microtome (Leica Microsystems Inc., Buffalo Grove, IL) at 50 nm and 70 nm thickness and collected on copper slot grids. Post-staining was done with 2% uranyl acetate in 50% ethanol and Sato's lead citrate (Hanaichi et al., 1986). Samples were analyzed with a CM12 TEM (FEI Electronics Instruments, Co., Mahwah, NJ) operated at 80kV and images were captured with a Gatan model 791 CCD camera (1024x1024 pixel area; Gatan Inc., Pleasanton, CA).

Tricyclazole assay and Thin Layer Chromatography (TLC)

Conidia of *A. fumigatus* wild type, *ayg1*^{Tn} and *mvp1*^{Tn} strains (10^4) were inoculated on the minimal medium with or without tricyclazole (30 µg/ml) for 3 days at 30°C before photographs of the colonies were taken. For the TLC experiment, same number of conidia (10^4) of wild type, *ayg1*^{Tn} and *mvp1*^{Tn} strains were spread over the plates containing the minimal medium with or without the supplement of tricyclazole (30 µg/ml). The cells were incubated at 30°C for 3 days and conidia were harvested with 1xPBS buffer. Conidia were then frozen by liquid nitrogen and then lyophilized. These lyophilized conidial samples were extracted using acetone using the same procedures as described previously (Tsai et al., 1999; Wheeler and Klich, 1995). The crude extracts were then spotted on TLC Silica gel 60 F₂₅₄ plates, developed in diethyl ether: hexanes:

formic acid (60:39:1) and visualized using UVP Bioimaging system under 254 overhead UV light.

Phylogenetic analysis of Mvp1 orthologues in various organisms

The software Clustal Omega (<http://www.ebi.ac.uk/Tools/msa/clustalo/>) was used to perform multiple alignment with default parameters(Sievers et al., 2011). The NCBI accession number for MVP1 homologs are listed below: XP_756052.1 (*A. fumigatus*), XP_680518.1 (*A. nidulans*), XP_002568982.1 (*Penicillium chrysogenum*), XP_002145139.1 (*Talaromyces marneffei*), XP_962901.2 (*Neurospora crassa*), NP_013717.1 (*Saccharomyces cerevisiae*), XP_571433.1 (*Cryptococcus neoformans*), NP_037453.1 (*Homo sapiens*), and XP_006504735.1 (*Mus musculus*).

Prediction of the subcellular localization of melanin biosynthetic enzymes in various fungal species

The Wolf PSORT(Horton et al., 2007), TargetP(Emanuelsson et al., 2000), and SignalP(Petersen et al., 2011) software were used to predict the subcellular localization of the melanin biosynthetic enzymes in various fungal species. The NCBI protein accession numbers for these homologs in the species listed in Table 1 are provided below. The homologs are presented in the same order as in Table 1. *A. fumigatus*: XP_756095.1; XP_756093.1; XP_756091.1; XP_756090.1; XP_756089.2; XP_756088.2. *A. clavatus*: XP_001276035.1; XP_001276034.1; XP_001276033.1; XP_001276032.1; XP_001276031.1; XP_001276030.1. *Penicillium marneffei*: XP_002147717.1; XP_002147709.1; XP_002147707.1; XP_002147705.1;

XP_002147704.1; XP_002147711.1. *Alternaria alternata*: AFN68292.1; AEH76761.1; BAD00089.1; ABO38546.1. *A. nidulans*: Q03149.2; CBF90107.1; XP_657750.1; CBF82394.1; XP_663001.1; XP_658505.1. *A. niger*: XP_001393884.2; XP_001393100.1; XP_001391270.1; XP_001401158.1; XP_001401160.2; XP_001389800.1. *Colletotrichum orbiculare*: ENH81867.1; Q00455.1; BAK57420.1; ENH77748.1; ENH77798.1; ENH81665.1. *Cochliobolus heterostrophus*: EMD96875.1/AAR90272.1; ABK63478.1; ABK63477.1; EMD88844.1; EMD94857.1; EMD95088.1 (low homology). *Sclerotinia sclerotiorum*: XP_001585805.1; XP_001585797.1; XP_001585798.1; XP_001597188.1; XP_001597433.1; XP_001586898.1 (low homology). *Botrytis cinerea*: CCD52428.1; CCD52437.1; CCD52436.1; CCD53247.1; XP_001558807.1; XP_001561053.1 (low homology). *Magnaporthe oryzae*: XP_003715434.1; XP_003712572.1; XP_003715430.1; XP_003720809.1; XP_003708928.1; XP_003716025.1. *Coprinopsis cinerea*: XP_001835415.2; XP_001839261.1; AAR01246.1 (low homology), AAR01249.1. *Sporisorium reilianum* SRZ2: CBQ71604.1; CBQ72575.1; CBQ67495.1; CBQ70142.1 (low homology)

The following are the locus names of the corresponding *A. fumigatus* melanin genes from the *Aspergillus* comparative genome website hosted by the Broad Institute (http://www.broadinstitute.org/annotation/genome/aspergillus_group/MultiHome.html) : Afu2g17600 (*pksP/alb1*), Afu2g17550 (*ayg1*), Afu2g17580 (*arp1*); Afu2g17560 (*arp2*), Afu2g17540 (*abr1*), and Afu2g17530 (*abr2*). We found that using sequences from either resources (NCBI or Broad) give the same subcellular prediction by these software programs except *Abr2*. Carefully analyses of the *Abr2* sequences from the two resources indicate an annotation of a longer version of *Abr2* from the Broad Institute. Our reverse transcription using primers designed for the disputed 5' region and internal regions of the *abr2* transcript only

detected shorter version of the transcripts, suggesting that the shorter version from NCBI is correct.

Inverse PCR, sequencing, Southern Blot, and gene knockout

The insertion site of the Ti plasmid in the *mvpI*^{Tn} mutant was identified using Inverse PCR. Genomic DNA from the *mvpI*^{Tn} strain was extracted following a standard procedure (Sambrook and Russell, 2006) and then digested with different restriction enzymes (*EcoRI* and *HindIII*) for 2-4 hours. The restriction enzyme digested products were ligated with the T4 DNA ligase. The ligated products were then used as templates for inverse PCR using 2 different primers set (M13F&AI76) and (LB-BO1&M13R). The PCR amplicons were then separated by gel electrophoresis and candidate bands were excised and purified using Qiagen gel purification system. The purified DNA was then subjected to sequencing using different primers at the Gene Technologies Lab (<http://www.idmb.tamu.edu/gtl/>). The insertion site at the *mvpI* open reading frame (ORF) was identified by BLAST of the obtained sequences against the *Aspergillus fumigatus* genome hosted by the Broad Institute (Galagan et al., 2005) (http://www.broadinstitute.org/annotation/genome/aspergillus_group/MultiHome.html). The single integration of the Ti plasmid at the *mvpI* locus in the *mvpI*^{Tn} mutant strain was verified by Southern blot analyses (Fig. S2). For Southern blot analyses, genomic DNA from these candidates was isolated using standard methods (Sambrook and Russell, 2006) and then digested with selected restriction enzyme. The probe used covered the T-DNA region of the Ti plasmid. The probe was labeled with ³²P using the Prime-It random primer labeling kit (Stratagene, Santa Clara, CA).

The *A. nidulans mvp1*Δ mutant was generated by homologous replacement of the native genetic locus with the *mvp1* deletion construct. This *mvp1* deletion construct was generated using the fusion PCR protocol as detailed below. A 1282 bp fragment upstream of the *mvp1* ORF and a 1323 bp fragment downstream of the *mvp1* ORF were fused to the 1999 bp *pyrG* marker amplified from the plasmid pFNO3 (Yang et al., 2004). This *mvp1* deletion construct was then used to transform the Asuku3 strain following the standard protoplasting method (Yelton et al., 1984).

Protein tagging

The GA5-eGFP-AfpYrG fragment amplified from the plasmid pFN03 (Yang et al., 2004) was used to construct the *Pmvp1-mvp1-eGFP*, *Pabr2-abr2-eGFP*, *Payg1-ayg1-eGFP*, *Parp1-arp1-eGFP*, and *Parp2-arp2-eGFP* by the same approach as previously described (Upadhyay et al., 2013). The *Pmvp1-mvp1-mCherry*, *PctpA-ctpA-mCherry*, and *Prab7-rab7-mCherry* fusion constructs were generated following the same procedures. The GA5-mCherry-tef-hyg fragment was generated by fusion PCR and mCherry was amplified from the plasmid pSK496 (Szewczyk and Krappmann, 2010). The *rab5* was tagged with mCherry at the N-terminus by fusion PCR to generate the *Prab5-mCherry-G6-rab5* construct. The construct containing the GA5-eGFP-AfpYrG flanked by the C-terminus of *alb1* ORF on the one side and the *alb1* ORF downstream fragment on the other was used to integrate GFP to the C-terminus of the *alb1* gene at its native locus.

Constructs *Panmvp1-anmvp1-chRFP*, *PwA-wA-GFP*, *PwA-wA-chRFP*, and *PyA-yA-chRFP* were generated following the same procedures. The GA5-GFP-pyroA and the GA5-

chRFP-pyroA fragment were amplified from the plasmid pHL85 and pHL86 respectively (Liu et al., 2009).

Light microscopy and fluorescence intensity quantification

Sample preparation and microscopic observation were performed essentially the same way as previously described (Chung et al., 2011). Images were acquired and processed with a Zeiss Axioplan 2 imaging system with an AxioCamMRm camera or a Zeiss Imager M2 with an AxioCam 506 camera. GFP was visualized using the filter FL filter set 38 HE EGFP while the mCherry/RFP was visualized using the filter FL filter set 43 HE Cy 3 (Carl Zeiss Microscopy). 40-50 conidia/strain were randomly selected to calculate the fluorescence intensity using the ZEN image software (Carl Zeiss Microscopy, NY). The distribution of the mean fluorescence intensity per conidium was plotted using the Origin9 software.

Protein extraction and western blotting

Proteins were extracted from young conidia of strains using the same procedure as previously described (Osherov and May, 1998). Aliquots of proteins were separated on SDS gels for western blot analyses using anti-GFP monoclonal antibody followed by a rabbit anti-mouse secondary antibody. Signal detection was performed using the ECL system according to the instruction provided by the manufacture (Pierce).

Supplemental References

Beauvais, A., Bozza, S., Kniemeyer, O., Formosa, C., Balloy, V., Henry, C., Roberson, R.W., Dague, E., Chignard, M., Brakhage, A.A., *et al.* (2013). Deletion of the α -(1,3)-glucan synthase genes induces a restructuring of the conidial cell wall responsible for the avirulence of *Aspergillus fumigatus*. *PLoS pathogens* 9, e1003716.

Butler, M.J., Gardiner, R.B., and Day, A.W. (2009). Melanin synthesis by *Sclerotinia sclerotiorum*. *Mycologia* 101, 296-304.

Chai, L.Y., Netea, M.G., Sugui, J., Vonk, A.G., van de Sande, W.W., Warris, A., Kwon-Chung, K.J., and Kullberg, B.J. (2010). *Aspergillus fumigatus* conidial melanin modulates host cytokine response. *Immunobiology* 215, 915-920.

Chung, D.W., Greenwald, C., Upadhyay, S., Ding, S., Wilkinson, H.H., Ebbole, D.J., and Shaw, B.D. (2011). *acon-3*, the *Neurospora crassa* ortholog of the developmental modifier, *medA*, complements the conidiation defect of the *Aspergillus nidulans* mutant. *Fungal Genet Biol* 48, 370-376.

Eisenman, H.C., Nosanchuk, J.D., Webber, J.B., Emerson, R.J., Camesano, T.A., and Casadevall, A. (2005). Microstructure of cell wall-associated melanin in the human pathogenic fungus *Cryptococcus neoformans*. *Biochemistry* 44, 3683-3693.

Emanuelsson, O., Nielsen, H., Brunak, S., and von Heijne, G. (2000). Predicting subcellular localization of proteins based on their N-terminal amino acid sequence. *J Mol Biol* 300, 1005-1016.

Galagan, J.E., Calvo, S.E., Cuomo, C., Ma, L.J., Wortman, J.R., Batzoglou, S., Lee, S.I., Basturkmen, M., Spevak, C.C., Clutterbuck, J., *et al.* (2005). Sequencing of *Aspergillus nidulans* and comparative analysis with *A. fumigatus* and *A. oryzae*. *Nature* 438, 1105-1115.

Hanaichi, T., Sato, T., Iwamoto, T., Malavasi-Yamashiro, J., Hoshino, M., and Mizuno, N. (1986). A stable lead by modification of Sato's method. *Journal of electron microscopy* 35, 304-306.

Horton, P., Park, K.J., Obayashi, T., Fujita, N., Harada, H., Adams-Collier, C.J., and Nakai, K. (2007). WoLF PSORT: protein localization predictor. *Nucleic Acids Res* 35, W585-587.

Jackson, J.C., Higgins, L.A., and Lin, X. (2009). Conidiation color mutants of *Aspergillus fumigatus* are highly pathogenic to the heterologous insect host *Galleria mellonella*. *PloS one* 4, e4224.

Liu, H.L., De Souza, C.P., Osmani, A.H., and Osmani, S.A. (2009). The three fungal transmembrane nuclear pore complex proteins of *Aspergillus nidulans* are dispensable in the presence of an intact An-Nup84-120 complex. *Molecular biology of the cell* 20, 616-630.

Oshero, N., and May, G.S. (1998). Optimization of protein extraction from *Aspergillus nidulans* for gel electrophoresis *Fungal Genetics Newsletter* 45, 38-40.

Petersen, T.N., Brunak, S., von Heijne, G., and Nielsen, H. (2011). SignalP 4.0: discriminating signal peptides from transmembrane regions. *Nature methods* 8, 785-786.

Sambrook, J., and Russell, D.W. (2006). *The condensed protocols from Molecular cloning : a laboratory manual* (Cold Spring Harbor, N.Y.: Cold Spring Harbor Laboratory Press).

Sievers, F., Wilm, A., Dineen, D., Gibson, T.J., Karplus, K., Li, W., Lopez, R., McWilliam, H., Remmert, M., Soding, J., *et al.* (2011). Fast, scalable generation of high-quality protein multiple sequence alignments using Clustal Omega. *Mol Syst Biol* 7, 539.

Spurr, A.R. (1969). A low-viscosity epoxy resin embedding medium for electron microscopy. *Journal of ultrastructure research* 26, 31-43.

Szewczyk, E., and Krappmann, S. (2010). Conserved regulators of mating are essential for *Aspergillus fumigatus* cleistothecium formation. *Eukaryotic cell* 9, 774-783.

- Tao, L., and Yu, J.H. (2011). AbaA and WetA govern distinct stages of *Aspergillus fumigatus* development. *Microbiology (Reading, England)* *157*, 313-326.
- Tsai, H.F., Fujii, I., Watanabe, A., Wheeler, M.H., Chang, Y.C., Yasuoka, Y., Ebizuka, Y., and Kwon-Chung, K.J. (2001). Pentaketide melanin biosynthesis in *Aspergillus fumigatus* requires chain-length shortening of a heptaketide precursor. *J Biol Chem* *276*, 29292-29298.
- Tsai, H.F., Wheeler, M.H., Chang, Y.C., and Kwon-Chung, K.J. (1999). A developmentally regulated gene cluster involved in conidial pigment biosynthesis in *Aspergillus fumigatus*. *Journal of bacteriology* *181*, 6469-6477.
- Upadhyay, S., Torres, G., and Lin, X. (2013). Laccases involved in 1,8-dihydroxynaphthalene melanin biosynthesis in *Aspergillus fumigatus* are regulated by developmental factors and copper homeostasis. *Eukaryotic cell* *12*, 1641-1652.
- van de Meene, A.M., Hohmann-Marriott, M.F., Vermaas, W.F., and Roberson, R.W. (2006). The three-dimensional structure of the cyanobacterium *Synechocystis* sp. PCC 6803. *Arch Microbiol* *184*, 259-270.
- Wheeler, M.H., and Klich, M.A. (1995). The effects of tricyclazole, pyroquilon, phthalide, and related fungicides on the production of conidial wall pigments by *Penicillium* and *Aspergillus* species. *Pesticide biochemistry and physiology* *52*, 125-136.
- Yang, L., Ukil, L., Osmani, A., Nahm, F., Davies, J., De Souza, C.P., Dou, X., Perez-Balaguer, A., and Osmani, S.A. (2004). Rapid production of gene replacement constructs and generation of a green fluorescent protein-tagged centromeric marker in *Aspergillus nidulans*. *Eukaryotic cell* *3*, 1359-1362.
- Yelton, M.M., Hamer, J.E., and Timberlake, W.E. (1984). Transformation of *Aspergillus nidulans* by using a trpC plasmid. *Proceedings of the National Academy of Sciences of the United States of America* *81*, 1470-1474.